

Novel Chitosan-Derived Nanomaterials and Their Micelle-Forming Properties

CAN ZHANG,^{†,‡} YA DING,[†] QINENG PING,[†] AND LIANGLI (LUCY) YU^{*,‡}

College of Pharmacy, China Pharmaceutical University, Nanjing 210009, P. R. China, and Department
 of Nutrition and Food Science, University of Maryland, 0112 Skinner Building, College Park,
 Maryland 20742

Six novel *N*-alkyl-*N*-dimethyl and *N*-alkyl-*N*-trimethyl chitosan derivatives were chemically synthesized and characterized using FT-IR, ¹H NMR, ¹³C NMR, differential scanning calorimetry (DSC), and X-ray diffraction spectrometry (XRD). The alkyl groups included octyl (C₈H₁₇-), decanyl (C₁₀H₂₁-), and lauryl (C₁₂H₂₅-). These chitosan derivatives were also evaluated for their micelle-forming properties using dynamic light scattering (DLS) and transmission electron microscopy (TEM) techniques. All six chitosan derivatives were capable of forming polymeric micelles in water with an average particle diameter ranging from 36 to 218 nm. Both *N*-octyl-*N*-dimethyl and *N*-octyl-*N*-trimethyl chitosan derivatives formed nanomicelles under the experimental conditions, with an average particle diameter of 36.0 and 52.5, respectively. Both the length of alkyl group and the *N*-trimethylation degree of the chitosan derivatives altered the size of their polymeric micelles. To further understand the effect of *N*-alkyl substitution degree of chitosan derivatives on size of their micelles, additional five *N*-octyl-*N*-trimethyl chitosan derivatives with *N*-alkyl substitution degree ranging from 8 to 58% were prepared and their micelle sizes were determined. The results showed that the diameter of the nanomicelles was proportional to the degree of *N*-octyl substitution. These data suggest that novel *N*-alkyl-*N*-dimethyl and *N*-alkyl-*N*-trimethyl chitosan derivatives may form nanomicelles. Additional research is required to further investigate the potential value-added utilization of these chitosan derivatives in controlled release and targeted delivery of hydrophobic bioactive food factors.

KEYWORDS: Chitosan; polymeric micelles; bioactive food factor; nutraceutical; functional food

INTRODUCTION

Nutraceuticals and functional foods are widely recognized for their potential in reducing the risk of aging-associated diseases and enhancing general human health. Development of nutraceuticals and functional foods is an emerging field in agricultural, food, and life sciences driven by current consumer desires of health promotion and disease prevention through improving diet (1–7). In 2004, the new IFT Expert Report provided a comprehensive review of functional foods and defined functional foods as “foods and food components that provide a health benefit beyond basic nutrition (for the intended population)” (3). An ideal functional food should have a number of characteristics including excellent sensory properties, efficacy, and safety. There are a number of challenges in research and development of nutraceuticals and functional foods such as poor bioavailability of hydrophobic bioactives, undesirable pharmacokinetic properties, loss of bioactivity due to degradation during food processing and storage, and undesirable sensory charac-

teristics. It has been suggested that nanotechnology may provide possible solutions to these challenges (8–10).

Nanotechnology is the science and technology that works at the atomic, molecular, and supramolecular levels at a scale of about 1–100 nm to better understand the relationships among macroscopic properties and molecular structure, degree of order, and intermolecular forces in synthetic materials and natural materials of botanical and animal origins (8–11). It is believed that nanotechnology may revolutionize current nutraceutical and food systems. These may include but are not limited to controlled release and targeted delivery of bioactive components, nanosensors and nanotracers for food safety and security, and nanomaterials from agricultural products and byproducts (9, 10, 12). Nanostructures capable of controlled release and targeted delivery of bioactives may greatly improve their stability, sensory properties, bioavailability and efficacy, safety and pharmacokinetic properties, and thus may lead to the renovation of nutraceuticals and functional foods. One of the essential steps for developing such nanostructures is to discover and develop novel self-assembling biocompatible and biodegradable polymer molecules. These self-assembling polymers may interact differently with individual bioactive factors with different chemical

* To whom correspondence should be addressed. Tel: (301) 405-0761. Fax: (301) 314-3313. E-mail: lyu5@umd.edu.

[†] China Pharmaceutical University.

[‡] University of Maryland.

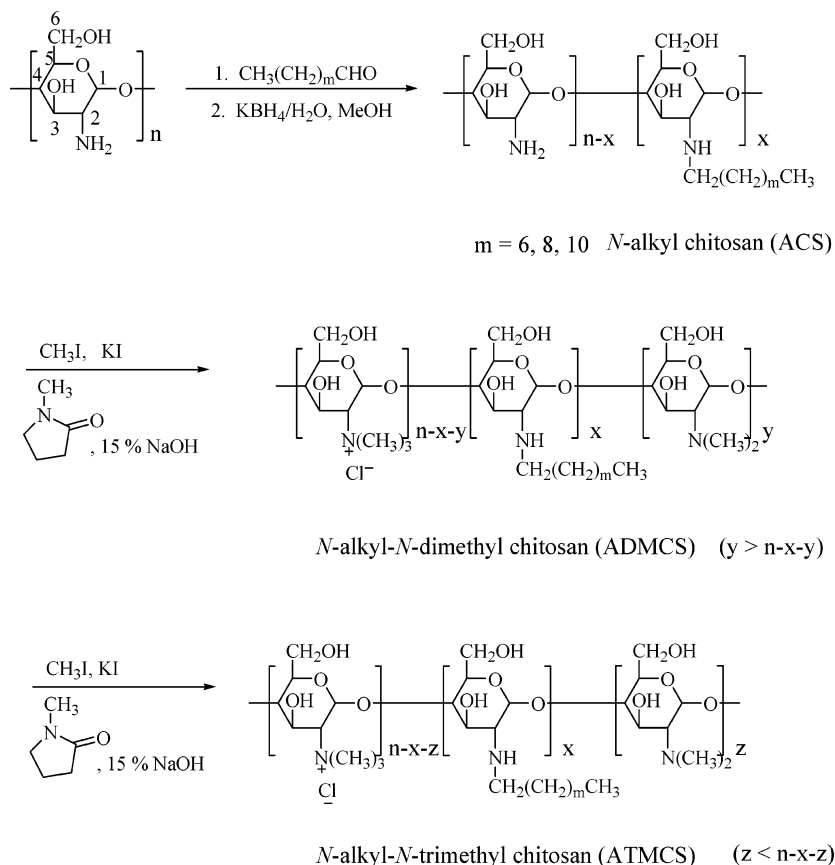


Figure 1. Synthesis of *N*-alkyl-*N*-dimethyl and *N*-alkyl-*N*-trimethyl chitosan derivatives.

and molecular structures. In other words, a number of such polymers capable of entrapping bioactive molecules with different chemical structures are required because of the structural diversity and huge number of bioactive food components such as flavonoids and ω -3 fatty acids.

Chitosan, a polymer of glucosamine, is a deacetylated product of chitin, which is a byproduct of crab and shrimp processing. The degree of deacetylation and molecular weight of chitosan determine its physical and chemical properties including rheological and aggregation properties (13, 14). Native chitosan preparations are used in supplemental products for their possible beneficial effects to humans such as hypolipidemic, antigonotoxic, and anticarcinogenic activities (13, 15). A few chitosan derivatives have been chemically synthesized and characterized for their possible utilizations in controlled release and targeted delivery of pharmaceuticals because chitosan is a nontoxic, biocompatible, biodegradable, and less expensive byproduct of the seafood industry (11, 14, 16–19). Some of these chitosan derivatives are self-assembling and able to form nanoparticles for controlled release and targeted delivery of bioactive components. These include *N*-alkyl-*O*-sulfate (18, 19), *O*-carboxymethylate (11), and cross-linked chitosan (11, 14), as well as chitosan derivatives containing hydrophobic branches on their backbone (16). *N*-alkyl-*O*-sulfate chitosan was able to form self-assembling nanomicelles and may be used as a vehicle for solubilization and slow release of paclitaxel, a hydrophobic anticancer compound (19). In addition, chemical modification may improve the mucoadhesive and penetration enhancing properties of chitosan (20). Utilization of chitosan derivatives for controlled release and targeted delivery of bioactives may promote the value-added use of crab and shrimp shells and enhance the profitability of the seafood industry.

In this study, a group of *N*-alkyl-*N*-dimethyl and *N*-alkyl-*N*-trimethyl chitosan derivatives with different degree of *N*-alkyl substitution and different chain length of the *N*-alkyl were synthesized. These chitosan derivatives were characterized using FT-IR, ^1H NMR, ^{13}C NMR, DSC, and XRD and evaluated for their micelle-forming properties. The results from this study may be used to promote the value-added utilization of chitosan and to improve the efficacy and safety of nutraceuticals and functional foods.

MATERIALS AND METHODS

Materials. Chitosan was provided by Nantong Suanglin Biochemical Co. Ltd. (Jiangsu, China) with a deacetylation degree of 97% and viscosity average molecular weight of 25 kDa. Pyrene (purity >99%) was purchased from Fluka Co. (Tokyo, Japan). All commercially available solvents and reagents were used without further purification.

Preparation of Novel Chitosan Derivatives. *N*-Alkyl-*N*-dimethyl and *N*-alkyl-*N*-trimethyl chitosan derivatives were prepared by introducing an alkyl group to NH_2 on C_2 of glucosamine unit in chitosan followed by a different degree of *N*-methylation as shown in **Figure 1**. *N*-Alkyl chitosan derivatives (ACS), including *N*-octyl (OCS), *N*-decanyl (DCS), and *N*-lauryl (LCS), were prepared following a laboratory procedure described previously (18). To prepare OCS, 1.0 g (5.6 mmol) of chitosan was suspended in 50 mL of methanol, and then 1 g (7.8 mmol) of octaldehyde was added in the suspension while stirring at room temperature. After 24 h of reaction, KBH_4 solution (0.5 g, 9.3 mmol in 5 mL of water) was slowly added to the reaction mixture. The resulting mixture was stirred at ambient temperature for another 24 h, followed by neutralization using 2 M hydrochloric acid. After precipitation with methanol, 0.96 g of OCS was collected by filtration, repeatedly washed with methanol and water, and dried at 60 $^\circ\text{C}$ overnight under a reduced pressure. The other two *N*-alkyl-substituted chitosan derivatives, DCS and LCS, were synthesized using

same molarity ratio of chitosan and decanal or lauryl aldehydes, respectively, and followed by KBH_4 reduction.

To prepare *N*-alkyl-*N*-dimethyl chitosan (ADMCS) derivatives, *N*-alkyl chitosan preparations were methylated according to a previously reported procedure with slight modification (21–23). For *N*-octyl-*N*-dimethyl chitosan (ODMCS), a mixture of 0.96 g (5.6 mmol) *N*-octyl chitosan, 2.4 g (16 mmol) sodium iodide, 5 mL of 15% (w/v) sodium hydroxide solution, and 15 mL (240 mmol) iodomethane in 15 mL *N*-methylpyrrolidone was mixed and reacted at 60 °C for 1 h with stirring. The resulting ODMCS was precipitated using ethanol and collected by centrifugation. After being washed with ethanol, the solid was dissolved in 5% (w/v) NaCl solution to exchange the iodide to ODMCS chloride. The crude ODMCS chloride was precipitated with ethanol and collected by centrifugation and then redissolved in distilled water and dialyzed against distilled water for 5 days using a membrane obtained from Sigma with a molecular weight cut off range of 10 000. The filtered solution was lyophilized, and 0.34 g of *N*-octyl-*N*-dimethyl chitosan (ODMCS) powder was obtained. DDMCS and LDMCS were prepared following the same procedure with same molarity ratio in the reaction. These ADMCS derivatives were tested for their micelle-forming properties and used to prepare ATMCS.

N-octyl-*N*-trimethyl chitosan (OTMCS) was prepared from ODMCS by further methylation. ODMCS (0.34 g) was dissolved in 15 mL of *N*-methylpyrrolidone containing 2.4 g (16 mmol) sodium iodide. A 5 mL volume of 15% sodium hydroxide solution and 3.2 mL (51 mmol) of iodomethane were added into the ODMCS methylpyrrolidone solution. After reacting at 60 °C for 30 min, an additional 1 mL (16.1 mmol) of iodomethane and 0.3 g of NaOH pellets were added to the mixture and stirred for another 1 h to complete the methylation reaction. OTMCS was precipitated with ethanol, collected by centrifugation, and purified following the same procedures described for ODMCS. OTMCS powder (0.2 g) was obtained. *N*-Decanal-*N*-trimethyl chitosan (DTMCS) and *N*-lauryl-*N*-trimethyl chitosan (LTMCS) were synthesized by following the same procedure.

Characterization of Chitosan Derivatives. FT-IR analysis was performed to evaluate the *N*-alkyl and *N*-methyl substitution. FT-IR spectra were recorded using a Fourier-transform infrared spectrometer in KBr discs (18).

^1H NMR and ^{13}C NMR spectra were also performed to evaluate the *N*-alkyl and *N*-methyl substitution and to determine the degree of trimethyl substitution (23). NMR was conducted using a Bruker (AVACE) AV-500 spectrometer. Chitosan was dissolved in the mixed solvent of D_2O and F_3CCOOD , while chitosan derivatives were dissolved in D_2O .

Elemental analysis was performed using an Element Vario EL III analyzer. Data from elemental analysis was used to calculate the degree of *N*-alkyl substitution.

Differential scanning calorimetry (DSC) and X-ray diffraction (XRD) spectrometry were employed to study the physical properties of chitosan and its derivatives. DSC was performed using the NETZSCH DSC 204 equipment with a temperature range of 30–550 °C and a heating rate of 20 °C/min. XRD spectra were obtained using an XD-3A powder diffraction meter with a $\text{Cu K}\alpha$ radiation range of 5–40° (2θ) at 40 kV and 30 mA.

Polymeric Micelle Size and Morphology. The micelles were prepared by dispersing chitosan derivatives in distilled water. After ultrasonication, the resulting solution was kept at ambient temperature in a sealed flask and subjected to further analysis of polymeric micelle size and morphology. The size and morphology of polymeric micelles were estimated according to the laboratory procedures previously described (19). Briefly, the size of the polymeric micelles was measured using the Zetasizer 3000HS instrument (Malvern Instruments, Malvern, U.K.) with 633 nm He–Ne lasers at 25 °C, and the concentration of micellar solution was 6 mg/mL. Transmission electron microscopy (TEM) analysis was performed using the micellar solution at 75 kV with an H-7000 (Hitachi, Japan) as described previously (19). The micellar solution was negatively stained with 0.01% phosphotungstic acid and placed on a copper grid coated with framer film.

Estimation of Critical Micelle Concentration. The critical micelle concentration of ODMCS was determined using pyrene (Fluka, >99%) as the hydrophobic fluorescent probe following a laboratory protocol

Table 1. Effects of the Alkyl Group and *N*-Trimethylation Degree on Micelle-Forming Properties of the Novel Chitosan Derivatives^a

derivative	length of alkyl group	trimethylation degree (%)	micelle size (nm)
ODMCS	8 – C	27	36
OTMCS	8 – C	74	52.5
DDMCS	10 – C	27	213
DTMCS	10 – C	74	218
LDMCS	12 – C	27	117
LTMCS	12 – C	74	128

^a ODMCS and OTMCS stand for *N*-octyl-*N*-dimethyl and *N*-octyl-*N*-trimethyl chitosan derivatives; DDMCS and DTMCS stand for *N*-decanyl-*N*-dimethyl and *N*-decanyl-*N*-trimethyl chitosan derivatives; LDMCS and LTMCS stand for *N*-lauryl-*N*-dimethyl and *N*-lauryl-*N*-trimethyl chitosan derivatives, respectively. The *N*-substitution degree of the *N*-alkyl group is 8% for all *N*-octyl-, -decanyl, and -lauryl chitosan derivatives shown in this table. Length of alkyl group is reported as the total carbon atoms in the alkyl group. Trimethylation degree was calculated using the integral of the ^1H NMR signals for the *N*-trimethylamino group ($\text{N}(\text{CH}_3)_3$) and that of the *N*-dimethylamino group ($\text{N}(\text{CH}_3)_2$). Micelle size is reported as the average diameter of micelles.

(19, 24). A known volume of pyrene in acetone (1.54×10^{-5} M, 400 μL) was placed in a flask. After removal of acetone using a rotary evaporator, 10 mL of aqueous polymer solution at each concentration (10^{-6} –2 mg/mL) was added into the flask. The resulting suspension was sonicated for 30 min at ambient temperature and kept at 65 °C for 3 h to equilibrate pyrene and the micelles. After being cooled at ambient temperature overnight, the micellar solution was filtered through a 0.22 μm membrane to remove the pyrene not trapped in the micelles. Fluorescence intensity was measured for micelles at an excitation wavelength of 339 nm and an emission wavelength ranging from 350 to 450 nm and was used to calculate the critical micelle concentration values for the selected newly synthesized chitosan derivative.

RESULTS AND DISCUSSION

A polymeric micelle is able to trap hydrophobic components in its hydrophobic core and enhance their water solubility because of its hydrophilic surface. Polymeric nanomicelles are well recognized as potential passive targeting carriers of anticancer agents because of their mechanical strength and small particle size (25, 26). Small particles are not captured by the reticuloendothelial cell systems (RES) and do not have “first-pass” effect and, consequently, may improve the bioavailability of entrapped bioactive components. The keys for developing such nanostructures are to (1) discover and develop novel self-assembling biocompatible and biodegradable polymers, (2) characterize their controlled release and targeted delivery potentials, (3) understand the physical, chemical, and mechanical mechanisms involved in their controlled release and targeted delivery functionalities, and (4) explore the relationship(s) between the molecular structure of polymers and their controlled release and targeted delivery behaviors, including the quantitative structure–functionality relationships. In this study, a group of *N*-alkyl-*N*-dimethyl and *N*-alkyl-*N*-trimethyl chitosan derivatives were synthesized. These chitosan derivatives were also characterized for their chemical structures and evaluated for their micelle-forming properties.

Synthesis and Characterization of the Chitosan Derivatives. Three *N*-alkyl-*N*-trimethyl chitosan (ATMCS) and three *N*-alkyl-*N*-dimethyl chitosan (ADMCS) derivatives were synthesized (Table 1). The alkyl groups included *n*- C_8H_{17} -, *n*- $\text{C}_{10}\text{H}_{21}$ -, and *n*- $\text{C}_{12}\text{H}_{23}$ -. The first important intermediate, *N*-alkyl chitosan (ACS), was prepared by introducing an alkyl group to the $\text{C}_2\text{-NH}_2$ of glucosamine units in chitosan (Figure 1). In this study, ACS was synthesized by reacting chitosan with the corresponding aldehyde followed by KBH_4 hydrogenation

of the Schiff's base (**Figure 1**). This was different from the method previously reported by Li and others (27). Li and others (27) prepared a number of *N*-alkyl chitosan derivatives with different chain lengths and substitution degrees by directly reacting chitosan with alkyl halide under alkaline conditions. In this study, *N*-alkyl derivatives with higher purity were obtained through the two step reactions, because the nucleophilic addition reaction has better selectivity. In contrast, the direct nucleophilic substitution reaction with alkyl halide may result in mixtures of *N*-alkyl and *O*-alkyl chitosan mixtures because alkyl halide may react with both NH_2 and OH groups. Although the NH_2 group has higher reactivity, there is only one possible NH_2 group in each glucosamine unit. In contrast, two OH groups are available in each glucosamine unit for the substitution reaction with alkyl halide. In 1996, Desbrieres and others prepared *N*-alkyl chitosan derivatives and investigated their rheological behaviors (28). The alkylation was accomplished by Schiff's base preparation followed by reduction using sodium cyanohydroborate (NaCNBH_4). NaCNBH_4 was selected because of its stability at acidic condition and its higher reactivity and selectivity than commonly used reducing agents including NaBH_4 . In this study, we were able to effectively reduce the iminium ion using KBH_4 as effective as that could be done with NaCNBH_4 . This may reduce the overall cost of preparation since NaBH_4 is less expensive than NaCNBH_4 . It needs to be pointed out that *N*-alkyl chitosans may act as absorption enhancers for bioactives besides simple intermediates for further preparation of *N*-alkyl-*N*-trimethyl chitosan (ATMCS) and three *N*-alkyl-*N*-dimethyl chitosan (ADMCS) derivatives.

ADMCS was prepared from ACS by methylation reactions on the primary amino group in the glucosamine unit accomplished by reacting ACS with iodomethane in the presence of strong base, while ATMCS was prepared under similar conditions by reacting ADMCS with iodomethane. The ADMCS and ATMCS derivatives with different percent trimethyl substitution were prepared by controlling the ratio of iodomethane and ACS or ACMCS, respectively, as well as altering the reaction duration. As shown in **Figure 1**, ATMCS derivatives carry a higher degree of positive charge at neutral pH than the corresponding ADMCS compounds, and the total charge of each molecule is less sensitive to environmental pH changes. On the other hand, ADMCS carries a lower degree of positive charge at neutral pH, whereas reduction of environmental pH increases the positive charge of each molecule because of the addition of proton onto the Me_2N -. Therefore, these two chitosan derivatives may differ in their micelle-forming properties. Furthermore, their micelles may have a different solubility in water and different applications in controlled release and targeted delivery of bioactive food components.

It has been reported that *N*-trimethyl chitosan chloride, an ATMCS derivative, exhibited excellent absorption-enhancing capacity across mucosal epithelia by opening epithelial tight-junctions (20, 22, 29). This absorption-enhancing capacity may be significantly altered by the degree of trimethyl substitution (22, 29). In addition to its role in nutrient and drug absorption, intestinal epithelial integrity is very important for prevention of toxic food factors such as viruses. Chitosan derivatives capable of opening epithelial tight-junctions may alter epithelial permeability and raise safety concerns. ADMCS and ATMCS with different degrees of *N*-trimethyl substitution may differ in their penetration-enhancing capacity due to their different epithelial tight-junction opening properties.

Structures of chitosan and its derivatives were first characterized using FTIR. All chitosan derivatives including ACS,

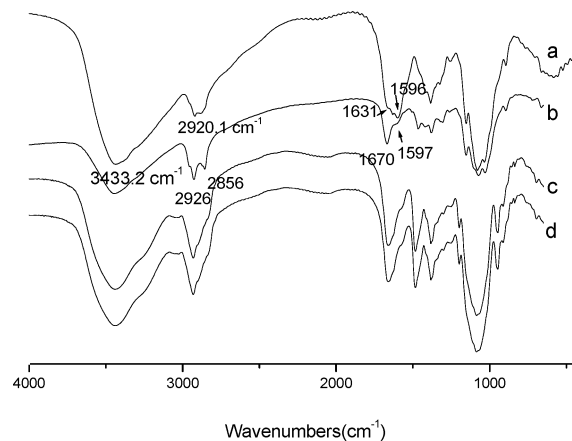


Figure 2. FT-IR spectra of chitosan derivatives: (a) chitosan; (b) *N*-octyl chitosan; (c) *N*-octyl-*N*-dimethyl chitosan; (d) *N*-octyl-*N*-trimethyl chitosan.

ADMCS, and ATMCS had peaks at 2957, 2858, 1467, 1380, and 800 cm^{-1} in the IR spectra which indicated the presence of an *N*-alkyl group. **Figure 2** shows the FTIR spectra of chitosan, *N*-octyl chitosan (OCS), *N*-octyl-*N*-dimethyl chitosan (ODMCS), and *N*-octyl-*N*-trimethyl chitosan (OTMCS). Chitosan had the strongest absorbance at 1597 cm^{-1} , which indicated the presence of the NH_2 group on C_2 of the glucosamine unit (**Figure 2a**). The intensity of this specific NH_2 signal was significantly decreased upon introducing the *N*-octyl group and was hardly observed for either *N*-octyl-*N*-dimethyl chitosan (ODMCS) or *N*-octyl-*N*-trimethyl chitosan (OTMCS) (**Figure 2b–d**). In a comparison of the FTIR spectra of chitosan and *N*-octyl chitosan, introducing the *N*-alkyl into the molecule increased intensities of peaks at 2856 and 2926 cm^{-1} (**Figure 2a,b**), suggesting the presence of *N*-alkyl substitution (27). New peaks were observed at about 1450 cm^{-1} in the FTIR spectra of *N*-octyl chitosan (OCS), *N*-octyl-*N*-dimethyl chitosan (ODMCS), and *N*-octyl-*N*-trimethyl chitosan (OTMCS) (**Figure 2**). Furthermore, the intensity of this peak was greater in the FTIR spectra of ODMCS and OTMCS than that observed for *N*-octyl chitosan under the same experimental conditions, designating the additional *N*-methyl substitution (**Figure 2b–d**). Similar FT-IR spectra were observed for other ACS, ADMCS, and ATMCS derivatives (data not shown). These data suggest the presence of methyl and long alkyl groups on nitrogen at the C_2 position of the glucosamine unit in chitosan molecules.

Figure 3 shows the ^1H NMR spectra of chitosan, ODMCS, and OTMCS. Compared to that of chitosan (**Figure 3a**), ODMCS had four additional peaks in their ^1H NMR spectra at 3.32, 2.46, 1.29, and 0.82 ppm (**Figure 3b**). The signal at 3.32 ppm was ^1H peaks of the trimethylamino group ($\text{N}(\text{CH}_3)_3$) and the α -methene group ($-\text{NHCH}_2(\text{CH}_2)_6\text{CH}_3$) of the *N*-octyl tail. The signals at 2.46 and 1.29 ppm were ^1H peaks of the dimethylamino group ($\text{N}(\text{CH}_3)_2$) and the other six methene groups of *N*-octyl group ($-\text{NHCH}_2(\text{CH}_2)_6\text{CH}_3$), respectively. The triple peaks at 0.82 were ^1H signals of the ω -methyl group in the *N*-octyl chain ($-\text{NHCH}_2(\text{CH}_2)_6\text{CH}_3$). In agreement with the FT-IR results, these four ^1H peaks suggested and confirmed the presence of *N*-octyl, *N*-dimethyl, and *N*-trimethyl groups in the synthesized chitosan derivatives. Furthermore, the ratio between the integral of the *N*-trimethylamino group ($\text{N}(\text{CH}_3)_3$) and that of the *N*-dimethylamino group ($\text{N}(\text{CH}_3)_2$) was approximately 2:1 (**Figure 3b**), which represents the degree of quaternization or positive charge of the ODMCS at neutral pH.

OTMCS had a ^1H NMR spectrum similar to that observed for ODMCS, except that the ^1H signal intensity of the trimethylamino group was stronger than that of the dimethylamino

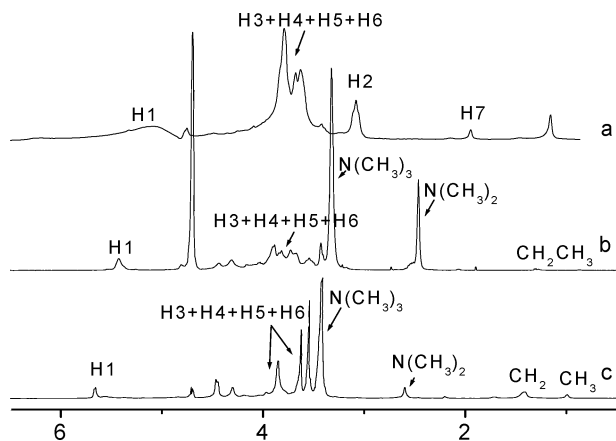


Figure 3. ^1H NMR spectra of (a) chitosan, (b) ODMCS, and (c) OTMCS. ODMCS and OTMCS represent *N*-octyl-*N*-dimethyl and *N*-octyl-*N*-trimethyl chitosan derivatives, respectively. The signal at 4.7 ppm was the solvent peak (D_2O), which may be eliminated from the ^1H NMR spectra using the zgpr pulse technique.

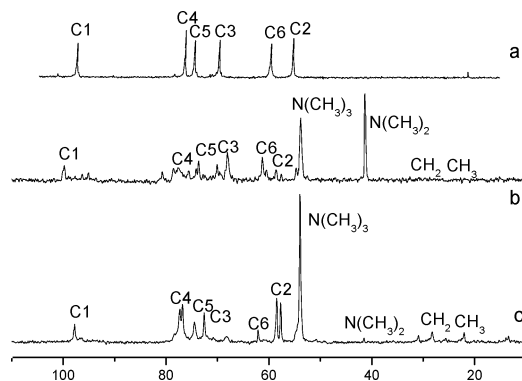


Figure 4. ^{13}C NMR spectra of (a) chitosan, (b) ODMCS, and (c) OTMCS. ODMCS and OTMCS represent *N*-octyl-*N*-dimethyl and *N*-octyl-*N*-trimethyl chitosan derivatives, respectively.

group (**Figure 3c**). The ratio between the integral of the *N*-trimethylamino group ($\text{N}(\text{CH}_3)_3$) and that of the *N*-dimethylamino group ($\text{N}(\text{CH}_3)_2$) was approximately 8:1. Taken together, the ^1H NMR data for ODMCS and OTMCS indicated that either ODMCS or OTMCS contains both *N*-dimethyl- and *N*-trimethylamino groups (**Figure 3b,c**). The difference was the relative amount of *N*-dimethyl- and *N*-trimethylamino groups in the chitosan molecule. This may be explained by the chemical mechanism involved in the NH_2 substitution reaction using CH_3I as the methylation agent. CH_3I has a poor selectivity between the secondary and the tertiary amino groups, $-\text{N}(\text{CH}_3)_2$ vs $-\text{N}(\text{CH}_3)_3$, respectively. Controlling the ratio of CH_3I to *N*-alkyl chitosan and the reaction duration are the only possible approaches to manipulate the relative amount of *N*-dimethyl- and *N*-trimethylamino groups in the methylation reaction products. However, none of these approaches can completely eliminate the formation of either *N*-dimethyl- or *N*-trimethylamino groups under the CH_3I methylation reaction conditions. Therefore, it is understandable that ODMCS has higher level of *N*-dimethylamino group as compared to the OTMCS, and the ratio of *N*-dimethyl- and *N*-dimethylamino groups in either ODMCS or OTMCS may vary and is highly dependent on the methylation reaction conditions.

The ^{13}C NMR analysis was performed to confirm the structures for *N*-alkyl, *N*-alkyl-*N*-dimethyl, and *N*-alkyl-*N*-trimethyl chitosan derivatives. **Figure 4** compares the ^{13}C NMR spectrum of ODMCS in D_2O with that of the chitosan in F_3 -

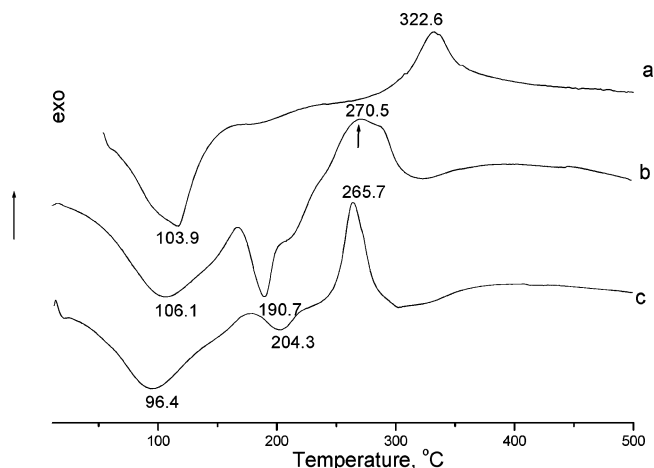


Figure 5. DSC thermograms of (a) chitosan, (b) ODMCS, and (c) OTMCS. ODMCS and OTMCS represent *N*-octyl-*N*-dimethyl and *N*-octyl-*N*-trimethyl chitosan derivatives, respectively.

$\text{CCOOD}/\text{D}_2\text{O}$. Characteristic ^{13}C NMR signals of glucosamine unit in chitosan were observed at 55.6 (C_2), 60 (C_6), 70 (C_3), 75 (C_5), 76.5 (C_4), and 97.5 (C_1) ppm (**Figure 4a**), which are in agreement with the previously reported data (30, 31). **Figure 4b** represents the ^{13}C NMR spectrum for ODMCS. The peak at 53.7 ppm was the ^{13}C signal for the trimethyl group ($-\text{N}(\text{CH}_3)_3$) and the α -methene group ($-\text{NHCH}_2(\text{CH}_2)_6\text{CH}_3$) in the *N*-octyl tail of the chitosan derivatives. The peak at 41.1 ppm was the ^{13}C signal for the dimethyl ($-\text{N}(\text{CH}_3)_2$) in the chitosan derivatives. The signals of the other six methene groups ($-\text{NHCH}_2(\text{CH}_2)_6\text{CH}_3$) and the methyl group at the end of *N*-alkyl tail ($-\text{NHCH}_2(\text{CH}_2)_6\text{CH}_3$) were shown at 34.3 and 23.9 ppm, respectively. The peaks at 99.6 (C_1), 77.5 (C_4), 77 (C_5), 68.4 (C_3), 61.1 (C_6), and 58.6 (C_2) ppm were ^{13}C signals of the corresponding carbon atoms of the glucosamine unit in chitosan molecule. These data confirmed the presence of *N*-octyl, *N*-dimethyl, and *N*-trimethyl groups in the ODMCS molecule, the newly synthesized chitosan derivative (**Figure 1**). In agreement with that observed in the ^1H NMR spectrum, the ^{13}C NMR data also support the conclusion that both *N*-trimethyl and *N*-dimethyl groups may be present in the *N*-alkyl-*N*-dimethyl chitosan preparations.

The ^{13}C NMR spectrum of OTMCS is similar to that for ODMCS, except that the ^{13}C signal intensity of the trimethyl group is stronger than that of dimethyl group (**Figure 4b,c**). The peaks at 97.9, 77.4, 74.6, 72.5, 58.5, 57.6, 54.2, 41.1, 28.1, and 22.1 represent the ^{13}C signals of C_1 , C_4 , C_5 , C_3 , C_6 , C_2 , $-\text{N}(\text{CH}_3)_3$, $-\text{N}(\text{CH}_3)_2$, CH_2 , and CH_3 , respectively.

DSC thermograms of chitosan and its *N*-octyl-*N*-dimethyl and *N*-octyl-*N*-dimethyl derivatives are shown in **Figure 5**. The spectrum of chitosan shows a broad endothermic peak at 103.9 °C and a sharp exothermic peak at 322.6 °C (**Figure 5a**). The presence of the endothermic peak may be explained by the elimination of moisture from the chitosan matrix. The exothermic peak might be attributed to the decomposition of the saccharine structure in chitosan. Similarly, the endothermic peaks at 106.1 °C for ODMCS and 96.4 °C for OTMCS may be due to the reduction of moisture content in the polysaccharides, whereas the endothermic peaks are at 190.7 °C for ODMCS and 204.3 °C for OTMCS (**Figure 5b,c**). The broad exothermic peaks at 270.5 °C for ODMCS and 265.7 °C for OTMCS correspond to their thermal decompositions. These data indicated that the introduction of substitution groups into chitosan molecules decreased their thermal stability and degree of order and improved their water solubility. The electronic

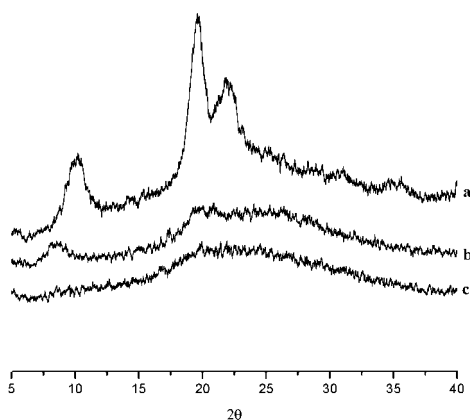


Figure 6. X-ray diffraction spectra of (a) chitosan, (b) ODMCS, and (c) OTMCS. ODMCS and OTMCS represent *N*-octyl-*N*-dimethyl and *N*-octyl-*N*-trimethyl chitosan derivatives, respectively.

repulsion of the positively charged amino groups and the steric effects of the *N*-alkyl tails and *N*-methyl groups in the different chitosan molecules may partially explain the different DSC spectra of chitosan, ODMCS, and OTMCS molecules.

X-ray diffraction analysis (XRD) was conducted for chitosan, ODMCS, and OTMCS to further evaluate their crystallization behaviors. Three reflection falls at 2θ of 11, 20, and 22° were observed in the X-ray diffraction spectrum of chitosan (**Figure 6a**), whereas ODMCS and OTMCS only had one broad peak at 2θ of about 20° (**Figure 6b,c**). It is well-accepted that the reflection fall at 2θ of 11° reflects the presence of crystal form I and the strongest reflection at 2θ of 20° corresponds to crystal form II (32). Taken together, the data in **Figure 6** indicated that introduction of *N*-alkyl, *N*-dimethyl, and *N*-trimethyl substitutions into chitosan molecules decreased their ability of forming intermolecular hydrogen bonds. In addition, these data suggested that both *N*-alkyl-*N*-dimethyl and *N*-alkyl-*N*-trimethyl chitosan preparations, ODMCS and OTMCS, were amorphous, which was supported by their DSC thermograms under the experimental conditions.

Particle Size and Morphology of the Polymeric Micelles.

The three *N*-alkyl-*N*-trimethyl (ATMCS) and the three *N*-alkyl-*N*-dimethyl chitosan derivatives (ADMCS) shown in **Table 1** were tested for their micelle-forming properties. All six tested chitosan derivatives were able to self-aggregate and form polymeric micelles in pure water under the experimental conditions. The diameter of the six polymeric micelles ranged from 36 to 218 nm (**Table 1**). Both chain length of the *N*-alkyl group and the degree of quaternization were able to alter the micelle forming properties of the *N*-alkyl-*N*-methyl chitosan derivatives. Both *N*-octyl-*N*-dimethyl and *N*-octyl-*N*-trimethyl chitosan derivatives formed polymeric nanomicelles, whereas the corresponding *N*-decanal (DDMCS and DTMCS) and *N*-lauryl (LDMCS and LTMCS) chitosan derivatives with the same trimethylation degree formed polymeric micromicelles with the diameters 2–5 times greater (**Table 1**). Interestingly, the polymeric micelles of both *N*-decanal-*N*-dimethyl and *N*-decanal-*N*-trimethyl chitosan derivatives had much larger particle size than the corresponding *N*-octyl and *N*-lauryl chitosan derivatives, suggesting that mechanisms involved in the micelle-forming behaviors of *N*-alkyl-*N*-dimethyl and *N*-alkyl-*N*-trimethyl chitosan derivatives are complicated. Further research is required to fully understand the relationship between the chemical structure of *N*-alkyl-*N*-di(tri)methyl chitosan derivatives and their micelle-forming properties. It is well-

Table 2. Effects of Hydrophobic Substitution Degree on Size of OTMCS Micelles^a

degree of <i>N</i> -octyl substitution	8%	20%	36%	48%	58%
size of blank micelle (nm)	52.5	58.2	78.5	80.5	101.2

^a OTMCS stands for *N*-octyl-*N*-trimethyl chitosan. All five OTMCS had a same ratio of 9:1 between their *N*-trimethyl ($N(\text{CH}_3)_3$) and *N*-dimethyl ($N(\text{CH}_3)_2$) amino groups. Micelle size is reported as an average diameter of micelles.

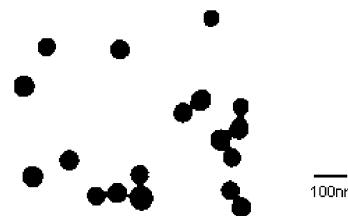


Figure 7. TEM micrograph of a blank OTMCS micelle ($\times 600\,000$). OTMCS represents *N*-octyl-*N*-trimethyl chitosan.

recognized that particle size is crucial for the in vivo fate of a drug delivery system (33). Understanding of the relationship between the chemical and molecular structures of the synthesized chitosan derivatives and the size of their possible polymeric micelles is very important to promote their potential utilization as carriers or nano- and microencapsulation agents for hydrophobic bioactive food factors and pharmaceuticals. To further investigate the effect of substitution degree of *N*-alkyl on micelle-forming properties of *N*-alkyl-*N*-di(tri)methyl chitosan derivatives, several *N*-octyl-*N*-methyl chitosan derivatives (OTMCS) with the same ratio of the *N*-trimethyl- and *N*-dimethylamino groups were prepared and tested for their micelle-forming properties. The results showed that the diameter of the nanomicelles was proportional to the degree of *N*-octyl substitution with a R^2 value of 0.94 by linear regression analysis (**Table 2**). Taken together, data in **Tables 1** and **2** indicate that *N*-alkyl-*N*-di(tri)methyl chitosan derivatives (ADMCS and ATMCS) are possible nanomicelle-forming materials and changes in the chemical structures may alter their micelle-forming properties. Additional studies are necessary to further investigate the structure–functionality relationships.

The TEM micrograph of the OTMCS micelles is presented in **Figure 7**, showing that OTMCS was able to form a near-spherical shape nanomicelle with slight deformation and aggregation. The size of the micelles was correlated well with that measured using the Zetasizer 3000HS instrument.

Critical Micelle Concentration. Critical micelle concentration is the minimum required concentration for a selected polymer to form micelles through self-assembling. Critical micelle concentration was determined for the *N*-octyl-*N*-dimethyl chitosan derivatives with an *N*-octyl substitution degree of 8% and a trimethyl substitution degree of 27% using the fluorescence method with pyrene as the probe. Pyrene is a hydrophobic molecule with poor water solubility and can be entrapped in the hydrophobic core of the ODMCS micelles in water. The fluorescence intensity was positively associated with the amount of pyrene in the ODMCS micelles, which reflects the level of micelles in the solution. The fluorescence intensity of pyrene in the micelles was obviously affected by ODMCS concentration (**Figure 8**). Below the critical micelle concentration, there were few micelles present in the polymer solution, which corresponded to the very low fluorescence intensity. Below certain concentration, increasing ODMCS concentration

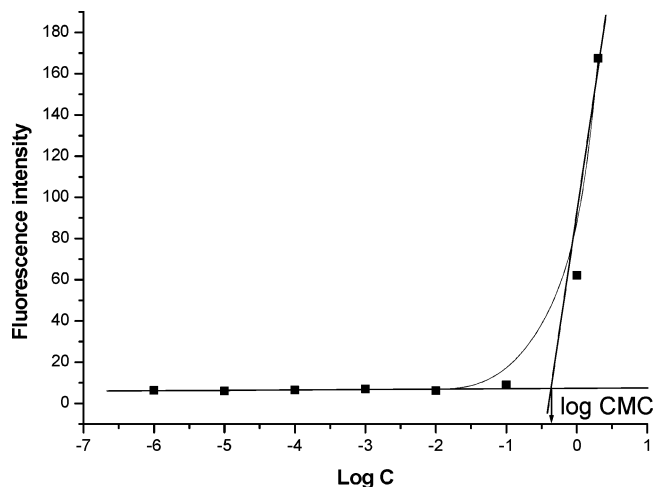


Figure 8. Fluorescent signal intensity of pyrene-containing ODMCS micelle (6×10^{-7} M) against ODMCS concentration. ODMCS stands for *N*-octyl-*N*-dimethyl chitosan. Cmc stands for the critical micelle concentration.

did not significantly elevate the fluorescence intensity. At or above a concentration point, a small increase of ODMCS concentration resulted in a sharp elevation of the fluorescence intensity. This concentration point is the critical micelle concentration for ODMCS, which was determined as 0.43 mg/mL under the experimental conditions (Figure 8).

In conclusion, novel *N*-alkyl-*N*-dimethyl and *N*-alkyl-*N*-trimethyl chitosan derivatives were chemically prepared from chitosan and characterized for their physicochemical properties. These chitosan derivatives are capable of forming polymeric micro- or nanomicelles and may serve as potential nanomaterials for encapsulation of hydrophobic bioactive factors. Additional research is required to further investigate the possible utilization of these chitosan-derived nanomaterials in controlled release and targeted delivery of bioactive food factors for improving the efficacy, stability, safety, sensory properties, and consumer acceptability and convenience of nutraceutical and functional food products, thus benefiting human health while promoting the value-added use of chitosan and enhance the profitability of seafood industry.

ACKNOWLEDGMENT

We thank Professor Wenbin Shen for recording the NMR spectra.

LITERATURE CITED

- Dreher, M. L. Functional Foods: Designing foods for improving health function: overview. *J. Nutraceut., Funct. Med. Foods* **1997**, *1*, 3–5.
- Simopoulos, A. P. Genetic variation and nutrition. *Food Rev. Int.* **1997**, *12*, 273–277.
- Clydesdale, F. Functional foods; opportunities & challenges. *Food Technol.* **2004**, *58* (12), 35–40.
- Sloan, A. E. The top 10 functional food trends 2004. *Food Technol.* **2004**, *58* (4), 28–51.
- IFIC. Functional foods attitudinal research. Aug. Intl. Food Information Council, Washington, DC, 2002; <http://ific.org/research/funcfoodsres02.cfm>.
- Ohr, L. M. Healthy aging. *Food Technol.* **2003**, *57* (3), 59–62.
- Schrooyen, P. M. M.; van der Meer, R.; Kruijff, C. G. De. Microencapsulation: its application in nutrition. *Proc. Nutr. Soc.* **2001**, *60*, 475–479.

- Ross, S. A.; Srinivas, P. R.; Clifford, A. J.; Lee, S. C.; Philbert, M. A.; Hettich, R. L. New technologies for nutrition research. *J. Nutr.* **2004**, *134*, 681–685.
- Roco, M. C. Nanotechnology: convergence with modern biology and medicine. *Curr. Opin. Biotechnol.* **2003**, *14*, 337–346.
- Moraru, C. I.; Panchapakesan, C. P.; Huang, Q.; Takhistov, P.; Liu, S.; Kokini, J. L. Nanotechnology: a new frontier in food science. *Food Technol.* **2003**, *57* (12), 24–29.
- Kumar, M. N. V. R. Nano and microparticles as controlled drug delivery devices. *J. Pharm. Pharmaceut. Sci.* **2000**, *3*, 234–258.
- Chen, H., Ed. Nanoscale science and engineering for agricultural and food systems, USDA Conference, Nov 18–19, 2002, Washington, DC; http://www.csrees.usda.gov/nea/technology/pdfs/nanoscale_10-30-03.pdf.
- Zhou, K.; Xia, W.; Zhang, C.; Yu, L. In vitro binding of bile acids and triglycerides by selected chitosan preparations and their physicochemical properties. *Lebensm.-Wiss. Technol.* **2006**, *39*, 1087–1092.
- Bodnar, M.; Hartmann, J. F.; Borbely, J. Preparation and characterization of chitosan-based nanoparticles. *Biomacromolecules* **2005**, *6*, 2521–2527.
- Koide, S. S. Chitin-chitosan: properties, benefits and risks. *Nutr. Res.* **1998**, *18*, 1091–1101.
- Agnihotri, S. A.; Mallikarjuna, N. N.; Aminabhavi, T. M. Recent advances on chitosan-based micro- and nanoparticles in drug delivery. *J. Controlled Release* **2004**, *100*, 5–28.
- Kosaraju, S. L. Colon targeted delivery systems: review of polysaccharides for encapsulation and delivery. *Crit. Rev. Food Sci.* **2005**, *45*, 251–258.
- Zhang, C.; Ping, Q.; Zhang, H.; Shen, J. Preparation of *N*-alkyl-*O*-sulfate chitosan derivatives and micellar solution of taxol. *Carbohydr. Polym.* **2003**, *54*, 137–141.
- Zhang, C.; Ping, Q.; Zhang, H. Self-assembly and characterization of paclitaxel-loaded *N*-octyl-*O*-sulfate chitosan micellar system. *Colloid Surf., B* **2004**, *39*, 69–75.
- Prabaharan, M.; Mano, J. F. Chitosan-based particles as controlled drug delivery systems. *Drug Delivery* **2005**, *12*, 41–57.
- Sieval, A. B.; Thanou, M.; Kotze, A. F.; Verhoef, J. C.; Brussee, J.; Junginger, H. E. Preparation and NMR characterization of highly substituted *N*-trimethyl chitosan chloride. *Carbohydr. Polym.* **1998**, *36*, 157–165.
- Kotze, A. F.; Thanou, M. M.; Luessen, H. L.; De Boer, A. G.; Verhoef, J. C.; Junginger, H. E. Enhancement of paracellular drug transport with highly quaternised *N*-trimethyl chitosan chloride in neutral environments: In vitro evaluation in intestinal epithelial cells (Caco-2). *J. Pharm. Sci.* **1999**, *88*, 253–257.
- Snyman, D.; Hamman J. H.; Kotze, J. S.; Rollings, J. E.; Kotze, A. F. The relationship between the absolute molecular weight and the degree of quaternisation of *N*-trimethyl chitosan chloride. *Carbohydr. Polym.* **2002**, *50*, 145–150.
- Kalyanasundaram, K.; Thomas, J. K. Environmental effects on vibronic band intensities in pyrene monomer fluorescence and their application in studies of micellar systems. *J. Am. Chem. Soc.* **1977**, *99*, 2039–2044.
- Yokoyama, M.; Miyauchi, M.; Yamada, N.; Okano, T.; Sakurai, Y.; Kataoka, K.; Inoue, S. Characterization and anticancer activity of the micelle-forming polymeric anticancer drug adriamycin conjugated poly (ethyleneglycol)-poly (aspartic acid) block copolymer. *Cancer Res.* **1990**, *50*, 1693–1700.
- Kataoka, K.; Kwon, G. S.; Yokoyama, M.; Okano, T.; Sakurai, Y. Block copolymer micelles as vehicles for drug delivery. *J. Controlled Release* **1993**, *24*, 119–132.
- Li, F.; Liu, W. G.; Yao, K. D. Preparation of oxidized glucose-crosslinked *N*-alkylated chitosan membrane and in vitro studies of pH-sensitive drug delivery behavior. *Biomaterials* **2002**, *23*, 343–347.
- Desbrieres, J.; Martinez, C.; Rinaudo, M. Hydrophobic derivatives of chitosan: Characterization and rheological behavior. *Int. J. Biol. Macromol.* **1996**, *19*, 21–28.

- (29) Thanou, M. M.; Kotze, A. F.; Scharringhausen, T.; Luessen, H. L.; De Boer, A. G.; Verhoef, J. C. Effect of degree of quaternization of *N*-trimethyl chitosan chloride for enhanced transport of hydrophilic compounds across intestinal Caco-2 cell monolayers. *J. Controlled Release* **2000**, *64*, 15–25.
- (30) Dung, P.; Milas, M.; Rinaudo, M.; Desbriers, J. Water soluble derivatives obtained by controlled chemical modifications of chitosan. *Carbohydr. Polym.* **1994**, *24*, 209–214.
- (31) Hiral, A.; Odani, H.; Nakajima, A. Determination of degree of deacetylation of chitosan by ¹H-NMR spectroscopy. *Polym. Bull.* **1991**, *26*, 87–94.
- (32) Samuels, R. J. Solid state characterization of the structure of chitosan films. *J. Polym. Sci., Polym. Phys. Ed.* **1981**, *19*, 1081–1105.
- (33) Moghimi, S. M.; Hunter, A. C.; Murray, J. C. Long-circulating

and target-specific nanoparticles: theory to practice. *Pharmacol. Rev.* **2001**, *53*, 283–318.

Received for review June 1, 2006. Revised manuscript received August 14, 2006. Accepted August 17, 2006. This research was supported by a grant of the Key Program of Science and Technology from the State Education Ministry of China with a SEMC Grant No. of 2003-03090, a grant from the Chinese Department of Science & Technology for International Science & Technology research cooperation with a Grant No. of 2005DFA30350, a grant from USDA National Research Initiatives with a federal Grant No. of 20043550314852, and a General Research Board Award from the Graduate School of the University of Maryland, College Park, MD 20742.

JF061541W